Experimental Neurology 321 (2019) 113030

Contents lists available at ScienceDirect

Experimental Neurology

journal homepage: www.elsevier.com/locate/yexnr

Research Paper

Reduced serotonin impairs long-term depression in basolateral amygdala complex and causes anxiety-like behaviors in a mouse model of perimenopause

Ya Wang[a,b], Yang Liu[c], Jianwei Xiong[c], Tingting Di[a,b], Zihao Yuan[b], Jie Wu[c,**], Ling Chen[a,b,*]

[a] State Key Laboratory of Reproductive Medicine, Nanjing Medical University, Nanjing 211166, China
[b] Department of Physiology, Nanjing Medical University, Nanjing 211166, China
[c] Department of Obstetrics and Gynecology, The First Affiliated Hospital of Nanjing Medical University, Nanjing 210029, China

ARTICLE INFO

Keywords:
Perimenopause
Anxiety-like behaviors
Basolateral amygdala complex
Serotonin
Long-term depression
Long-term potentiation

ABSTRACT

Perimenopause is characterized by a gradual depletion of ovarian follicles with increased vulnerability to anxiety. However, the underlying mechanisms remain poorly understood. Herein, we show that chronic exposure to 4-vinylcyclohexene diepoxide (VCD) in adult female mice (VCD-mice) caused follicles depletion and decline of serum estradiol (E2) and progesterone levels. Serotonin (5-HT) synthesis in dorsal raphe nucleus (DRN) and serotonergic afferents to basolateral amygdala complex (BLA) were reduced in VCD-mice, which were recovered by the supplement E2. VCD-mice appeared anxiety-like behaviors, which was relieved by the treatment with E2 or the co-administration of 5-HT1Ar agonist 8-OH-DPAT and 5-HT2A/Cr agonist DOI. The bath-application of 8-OH-DPAT in the slices obtained from VCD-mice (VCD-slices) corrected the increase in presynaptic glutamate release at external capsule-BLA synaptic transmission. Threshold to induce NMDA receptor (NMDAr)-dependent long-term potentiation (LTP) was declined in VCD-mice with elevation of CaMKII phosphorylation, which was sensitive to 8-OH-DPAT. Notably, the bath-application of 8-OH-DPAT in VCD-slices caused a decrease in the GABAergic feedback inhibition, which was restored by adding DOI. In addition, NMDAr-independent long-term depression (LTD) could not be induced in VCD-mice, which was rescued by the co-application of 8-OH-DPAT with DOI or the $GABA_A$ receptor agonist muscimol. Furthermore, the treatment of VCD-mice with E2 could prevent the facilitation of LTP and recover the LTD induction. Thus, the results indicate that the 5-HT deficiency in the BLA of VCD-mice causes the facilitation of LTP *via* enhanced glutamate release and impairs the LTD induction through diminished GABAergic inhibition, leading to anxiety-like behaviors.

1. Introduction

Perimenopause, a transition period from reproductive (premenopause) to non-reproductive (postmenopause) life in women (Harlow et al., 2012), is characterized by a gradual depletion of ovarian follicles leading to a dynamic and complex hormonal milieu and is associated with increased vulnerability to anxiety (Bryant et al., 2012; Prior, 2011). Several lines of evidence suggest that after puberty mental disorders are most frequent during perimenopause (Deecher et al., 2008). Although perimenopause has been considered to be a period associated with increased risk for anxiety and mood symptoms in women, the underlying mechanisms remain poorly understood.

Both epidemiological and clinical studies have consistently reported that estradiol (E2) therapy is effective in attenuating many of perimenopausal symptoms, including mood disorders. Although the level of E2 is not reduced significantly at early perimenopause period (Santoro and Randolph Jr., 2011), there is a significant decline of E2 level at late perimenopause period (Burger et al., 1995; Santoro and Randolph Jr.,

Abbreviations: 5-HT, serotonin; ACSF, artificial cerebrospinal fluid; AOF, accelerated ovarian failure; BLA, basolateral amygdala complex; CaMKII, calmodulin-kinase II; DMSO, dimethylsulfoxide; DRN, dorsal raphe nucleus; EPM, elevated plus-maze test; EPSPs, excitatory postsynaptic potentials; E2, estradiol; $GABA_AR$, $GABA_A$ receptor; HE, hematoxylin and eosin; HFS, high-frequency stimulation; IPI, interpulse interval; LFS, low-frequency stimulation; LTD, long-term depression; LTP, long-term potentiation; NMDAr, NMDA receptor; OFT, open-field test; PPF, Paired-pulse facilitation; PPI, paired-pulse inhibition; PPR, paired-pulse ratio; P4, progesterone; TPH, tryptophan hydroxylase; VCD, 4-vinylcyclohexene diepoxide; VCD-mice, mice model of perimenopause induced by VCD

* Correspondence to: L. Chen, Department of Physiology, Nanjing Medical University, Longmian Road 101, Nanjing 211166, China.
** Corresponding author.
E-mail addresses: wujiemd@126.com (J. Wu), lingchen@njmu.edu.cn (L. Chen).

https://doi.org/10.1016/j.expneurol.2019.113030
Received 20 October 2018; Received in revised form 7 July 2019; Accepted 31 July 2019
Available online 01 August 2019

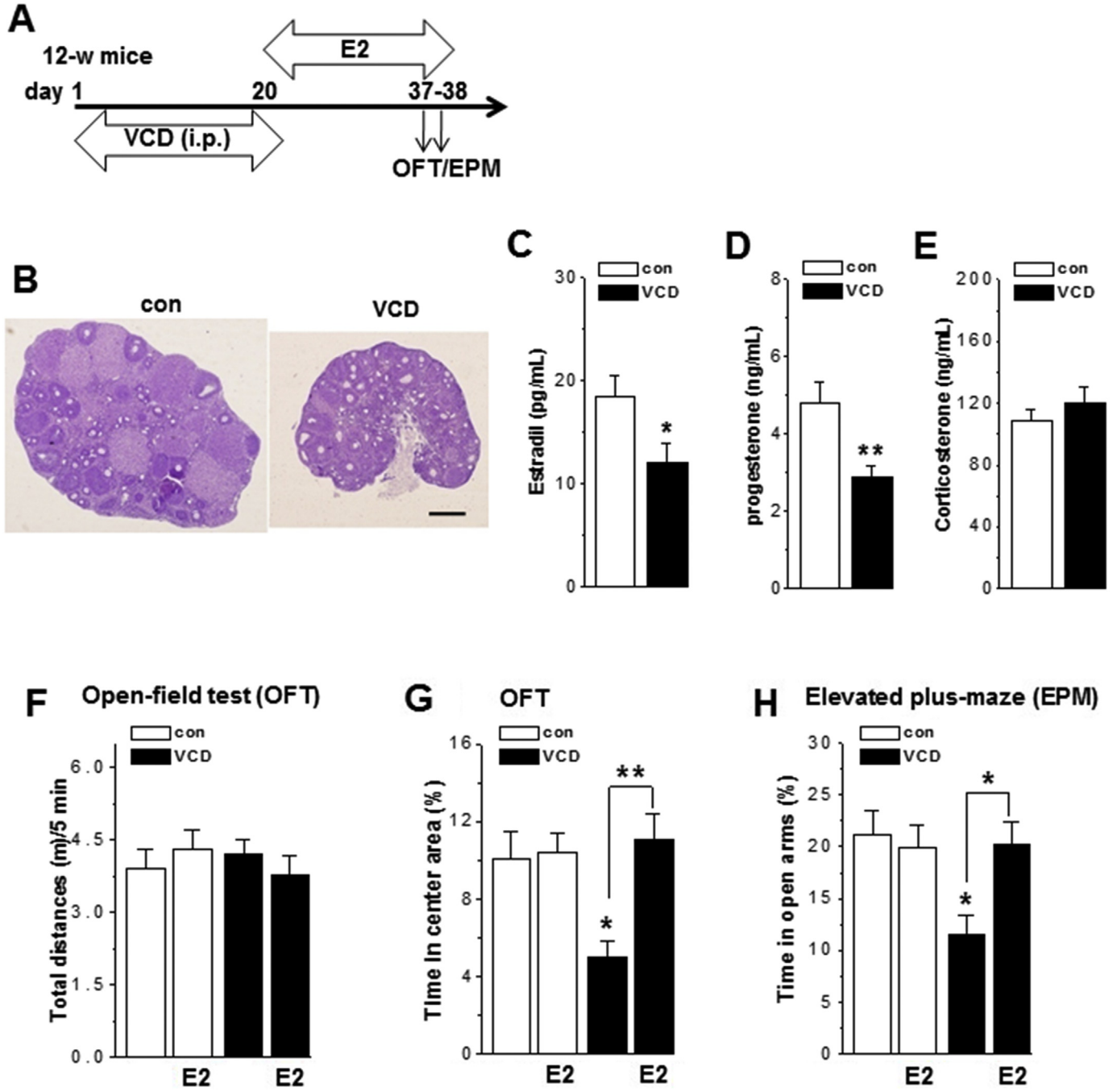

Fig. 1. VCD-accelerated ovarian failure in mice induces anxiety-like behaviors. (A) Experimental timeline. Horizontal arrow indicates the time (day) of VCD injection and E2 administrated after stopping VCD; ↓: time of open-field test (OFT) and elevated plus-maze test (EPM) performance. (B) Representative pictures of ovaries stained by HE in control mice and VCD-mice. Scale bars = 200 μm. (C–E) Bar graphs show the mean level of serum estradiol, progesterone and plasma corticosterone in control mice and VCD-mice. $*p < 0.05$ and $**p < 0.01$ (Student's *t*-test). (F&G) Bars show the distance traveled (m) and the time spent in the central portion (%) during the OFT in control mice and VCD-mice treated with E2. $*p < 0.05$ and $**p < 0.01$ (two-way ANOVA). (H) Bar graph shows the time spent in the open arms of EPM (%). $*p < 0.05$ (two-way ANOVA).

2011). Chronic exposure to 4-vinylcycloxene diepoxide (VCD) in rodents specifically causes apoptosis of primary and primordial follicles to model perimenopause in women (Mayer et al., 2002). The model of perimenopause induced by VCD is termed the accelerated ovarian failure (AOF) model (Brooks et al., 2016). There is increasing evidence suggesting a relationship between anxiety and gonadal hormones (Toufexis et al., 2006). The rat treated with VCD shows anxiety-like behavior with a decline in plasma level of progesterone rather than E2 and corticosterone (Reis et al., 2014). Although VCD does not cross the blood-brain barrier (Van Kempen et al., 2011), the treatment with VCD in rats reduced remarkably the activity of tryptophan hydroxylase (TPH), a rate-limiting enzyme in serotonin (5-HT) synthesis in the dorsal raphe nucleus (DRN), and the level of serotonin in the amygdale, which was recovered by the supplement of E2 (Pestana-Oliveira et al., 2018). The serotonergic system has long been implicated in anxiety disorders. For example, 5-HT1A receptor (5-HT1Ar) knockout mice exhibited anxiety-like behaviors (Ramboz et al., 1998). Several lines of evidence have indicated the anxiolytic-like effects of 5-HT and 5-HT receptor agonists in human and rodents (Gleason et al., 2015; Waider et al., 2011).

The anxiety-related behaviors are well known to enhance fear response in aversive environments and to facilitate fear memory (Gross et al., 2000). The basolateral nucleus of the amygdala (BLA) is considered to be a critical nucleus for fear responses in rodents and humans (File et al., 1998; Zhang et al., 2017). Synaptic plasticity, long-term potentiation (LTP) and long-term depression (LTD) in the BLA may underlie the acquisition, consolidation and extinction of fear memories. There are two major types of glutamatergic principal neurons and GABAergic interneurons in the BLA. The fear memory formation depends on the induction of LTP in the BLA principal neurons (Goosens and Maren, 2002), while the production of LTD is thought to promote the extinction of learned fear (Kim et al., 2007). Several laboratories have demonstrated that the GABAergic system in amygdaloid networks is involved in generating responses to fear-conditioned stimuli (Ehrlich et al., 2009; Sangha et al., 2009). A large body of evidence has established that the neuronal activity and synaptic plasticity in the BLA are regulated by the feedforward and/or local feedback circuitry between principal neurons and interneurons. The activation of presynaptic 5-HT1Ar reduces glutamate release (Bobker and Williams, 1989). The 5-HT2r agonist directly activates GABAergic interneurons in the BLA (Rainnie, 1999). Therefore, it is of great interest to investigate whether the VCD-reduced 5-HT in the BLA alters the excitation-inhibition circuitry to affect the induction of synaptic plasticity.

The aim of this study is to clarify the mechanisms underlying VCD-accelerated ovarian failure to induce anxiety-related behaviors. We investigated the influence of VCD-accelerated ovarian failure in the 5-HT synthesis, the synaptic properties and plasticity in the BLA. We further determined the association of the VCD-reduced 5-HT with the alteration of synaptic properties and plasticity, and the production of anxiety-related behaviors and explored the underlying mechanisms.

2. Materials and methods

2.1. Experimental animals

The procedures involving animals and their care were conducted in conformity with the ARRIVE guidelines of Laboratory Animal Care (Kilkenny et al., 2011). This animal study was approved by the Institutional Animal Care and Ethical Committee of the Nanjing Medical University. All animal experiments were performed in accordance with the guidelines of the Laboratory Animal Research Institute of Nanjing Medical University. Twelve-week-old female mice (28.8 ± 1.5 g) (ICR, Oriental Bio Service Inc., Nanjing) were maintained in the Animal Research Center of Nanjing Medical University (temperature 23 ± 2 °C, humidity 55 ± 5%, 12:12 h light/dark cycle) with free access to food and water. All mice were randomly assigned to 3 experimental groups. (1) The behavioral tests and immunohistochemistry or RT-PCR analyses were sequentially performed in the same cohorts. (2) The electrophysiological tests were performed in other experimental groups. (3) The Western blot analyses were performed after 10 min of electrophysiological conditioning stimulation.

2.2. Preparation of the accelerated ovarian failure (AOF) model

VCD (Sigma-Aldrich) was diluted in corn oil and administrated by intraperitoneal injections daily at a dose of 160 mg/kg (1.5 μl/g body weight) for 20 consecutive days (Mark-Kappeler et al., 2011). The mice were injected with corn oil at the same volume served as the control group. By vaginal cytology at 0800–0900, estrous cyclicity was monitored daily (Wang et al., 2018) to observe a prolongation of cycle length during this time frame of impending ovarian failure (data not shown). The mice at day 18 after the cessation of VCD or the control mice at diestrus were anesthetized with an injection (i.p.) of pentobarbital (50 mg/kg) (Fig. 1A). Both dissected ovaries were fixed in Bouin's fluid. The ovaries were dehydrated through a graded series of alcohol, cleared in xylene, and then embedded in paraffin wax. The ovaries sections (5 μm) were cut, then deparaffined and rehydrated. The sections were stained with hematoxylin and eosin (HE). We observed the ovaries sections using a conventional light microscope (Olympus DP70, Japan) with a 40× objective.

2.3. Measurement of hormones

Orbital blood (~100 μl) was obtained from mice anesthetized with chloral hydrate (400 mg/kg, i.p.) at 1600–1700. Serum were separated by centrifugation at 4 °C and stored at −80 °C until assayed. The measurement of serum E2, progesterone (P4) and corticosterone using commercial enzyme-linked immunosorbent assay (ELISA) kits (Uscn Life Science Inc., Houston, TX, USA) was repeated 3 times. The intra and interassay coefficients of variation were 6% and 5.8% for E2, 6.2% and 11.8% for P4, 4.8% and 6.35% for corticosterone, respectively. The lowest detectable levels were 4.45 pg/ml for E2, 0.47 ng/ml for P4 and 0.57 ng/ml for corticosterone.

2.4. Drug administration

The 5-HT1Ar agonist 8-OH-DPAT, the 5-HT1Ar antagonist WAY-100635, and the 5-HT2r antagonist sarpogrelate were purchased from MCE (Monmouth Junction, NJ, USA). The 5-HT1Br agonist CGS-12066B maleate (CGS) and the 5-HT2A/Cr agonist 2,5-dimethoxy-4-iodoamphetamine (DOI) was purchased from Tocris (Minneapolis, MN, USA). The $GABA_A$ receptor ($GABA_AR$) agonist muscimol, the $GABA_A$ receptor ($GABA_AR$) antagonist bicuculline methiodide (bicuculline), the NMDA receptor (NMDAr) antagonist AP-V, the NMDAr channel blocker MK801 were purchased from Sigma (St. Louis, MO, USA). These drugs were dissolved in dimethylsulfoxide (DMSO) and then were diluted by artificial cerebrospinal fluid (ACSF) (in mM: 124 NaCl, 2 $CaCl_2$, 4.5 KCl, 1 $MgCl_2$, 26 $NaHCO_3$, 1.2 NaH_2PO_4, and 10 D-glucose, pH 7.4) to a final DMSO concentration of 0.1%. For *in vivo* treatment, the mice were given daily the subcutaneous (s.c.) or intraperitoneal (i.p.) injection of 8-OH-DPAT (0.5 mg/kg), CGS (10 mg/kg) and DOI (2.5 mg/kg) (Khatri et al., 2014; Li et al., 2010). The VCD-mice received a subcutaneous implant of a Silastic capsule (Dow Corning, Midland, MI, USA) containing 0.625 μg E2 (in sesame oil, Sigma-Aldrich Corp.) to produce a physiological level of serum E2 (Wang et al., 2014). For the bath-application of the slices, the slices were perfused with 8-OH-DPAT (5 μM), WAY-100635 (40 nM), CGS (20 μM), DOI (10 μM), sarpogrelate (1 μM), muscimol (10 μM), bicuculline (10 μM) , AP-V(50 μM) or MK801 (10 μM) (Chen et al., 2016; Itoh and Kajikuri, 2011; Jang et al., 2010; Rainnie, 1999).

2.5. Behavior analysis

Open-field test (OFT) and elevated plus-maze test (EPM) were used to evaluate spontaneous activity and anxiety-like behaviors spaced with at least 24 h. The behavioral data were recorded by a video recorder (Winfast PVR; Leadtek Research Inc., Fremont, CA, USA) and analyzed using TopScan Lite 2.0 (Clever Sys, Reston, VA, USA).

2.5.1. Open-field test (OFT)

Each mouse was placed in a clear, open-top, square Plexiglas box (60 cm × 60 cm × 40 cm) with 15 lx lighting and allowed to freely explore for 5 min. We measured the traveled distance and the time spent in the center region of the arena (Dere et al., 2004).

2.5.2. Elevated plus-maze (EPM)

The maze consisted of two open arms painted white (23.5 cm × 8 cm × 20 cm high) and two enclosed arms painted black (23.5 cm × 8 cm × 20 cm high) with a 15 lx lighting (Gundersen et al., 2013). The apparatus was raised to a height of 38.5 cm above the floor. Mice were placed in the center area facing one of the open arms. In the elevated pulse-maze test, the number of open arms entering and

keeping time were recorded for 5 min.

2.5.3. Forced swim test (FST)

Each mouse was placed in a glass cylinder (300 mm high, 280 mm in diameter) filled with water to a height of 20 cm (25 ± 1 °C). Mice were subjected to a 6 min swimming test. Total immobility time was calculated as the minimal movements that were required to keep the head above water (Zhang et al., 2017).

2.5.4. Tail suspension test (TST)

Mice were suspended by the tail using adhesive tape to a rod 60 cm above the floor as described previously (Zhang et al., 2017). The trials were conducted for 6 min, during which the duration of immobility was recorded.

2.6. Immunohistochemistry for TPH

Mice anesthetized with pentobarbital (50 mg/kg, i.p.) were transcardially perfused with ice-cold 4% paraformaldehyde. The brains were transferred and fixed overnight in 4% paraformaldehyde. Brains were transferred into 15% and 30% sucrose. The coronal sections (30 μm) of rostra DRN, mid DRN (Pestana-Oliveira et al., 2018) and BLA (Zhang et al., 2017) were cut using a cryostat (Leica CM3050S; Leica Microsystems, Germany). The sections were incubated in 1% hydrogen peroxide for 10 min and were subsequently treated with 1% BSA (Sigma Chemical Co) for 60 min to block non-specific binding. The sections were incubated with sheep anti-TPH polyclonal antibody (1:2000; Millipore) for 40 h at 4 °C. The sections were subsequently treated with biotinylated rabbit anti-sheep IgG (1:600; Vector Laboratories) at room temperature for 1 h. Immunoreactivities were visualized using an avidinbiotin horseradish peroxidase complex (Vector Laboratories, Burlingame, CA, USA). The TPH positive cells and fibers were observed using a conventional light microscope (40 × objective, DP70; Olympus).

2.7. Electrophysiological analysis

2.7.1. Slice preparations

Coronal slices were prepared as previously described (Yang et al., 2017). In brief, the animals were deeply anesthetized with isoflurane, decapitated and the brains were rapidly removed. Tissue blocks containing the BLA were mounted on a Vibratome (Microslicer DTK 1500, Dousaka EM Co, Kyoto, Japan) in a chamber filled with cold cutting solution composed of (in mM) 94 sucrose, 30 NaCl, 4.5 KCl, 1.0 $MgCl_2$, 26 $NaHCO_3$, 1.2 NaH_2PO_4, and 10 D-glucose, pH 7.4. Coronal brain slices were cut at 400 μm thickness and transferred to an interface chamber where they were maintained at 32 ± 1 °C and perfused continuously with oxygenated ACSF. The slices were allowed to rest for at least 1 h after the preparation, before recording.

2.7.2. Field potential recording

A bipolar tungsten electrode was positioned in outside of the BLA to stimulate the external capsule (EC) fibers from the cortex. A 5-MΩ resistance glass microelectrode was filled with 2 M NaCl and positioned in inside of the BLA. Field excitatory postsynaptic potentials (EPSPs) were measured by the glass microelectrode and connected to a neutralized, high input-impedance preamplifier with a high-pass filter at 5 kHz. Signals were amplified with the use of a differential AC amplifier (A-M Systems, model 1700, Seattle, WA) and were digitized and saved using the pCLAMP system (Axon Instrument Inc., CA, USA). Stimulus intensities were adjusted to evoke half maximal EPSP. The baseline response was obtained at intervals of 15 s. Paired-pulse facilitation (PPF) and paired-pulse inhibition (PPI) were induced by paired-pulse stimulation with an interpulse interval (IPI) of 50–100 ms and 20–30 ms, respectively. The paired-pulse ratio (PPR) was calculated with the following formula: $(EPSP_{S2}/EPSP_{S1}) \times 100$. After the stabilization of baseline response for at least 10 min, high-frequency stimulation (HFS) was applied to induce LTP. The HFS consisted of 100 pulses at 100 Hz with the test stimulus intensity, which was applied one time (HFS × 1) or five times (20 s interval; HFS × 5) (Li and Rainnie, 2014). LTD was induced by delivering low-frequency stimulation (LFS, 1 Hz 15 min). The EPSP was recorded for 60 min after the conditioning stimulation. LTP or LTD was determined if the EPSP slopes were greater or lower than 20% of baseline at 55–60 min after delivering HFS or LFS.

2.8. Western blot analysis

At 10 min after HFS × 1 was delivered, the tissues of BLA were immediately micro-dissected and stored at −80 °C until assayed. The tissues of BLA were homogenized in 1% Nonidet P-40 lysis buffer containing 50 mM Tris, 150 mM NaCl, 0.02% NaN_3, and complete protease inhibitors (Roche). The homogenates were centrifuged for 15 min at 12,000 r.p.m. (Thermo Scientific) and the supernatants were collected. Protein concentrations were determined using a bicinchoninic acid (BCA) protein assay kit (Pierce). The proteins (20 μg) were separated by SDS-polyacrylamide gel electrophoresis (SDS-PAGE) and transferred to a polyvinylidene fluoride membrane. The membranes were incubated with 5% nonfat dried milk at room temperature for 60 min and then incubated in the rabbit polyclonal antibody of GluN2B phosphorylation (1:1000; Abcam, Cambridge, UK), or the rabbit monoclonal antibodies of CaMKII and GluR1 phosphorylation (1:1000; Cell Signaling Technology, Boston, MA, USA) at 4 °C overnight. The membranes were incubated with HRP-labeled secondary antibodies and developed using an ECL detection Kit (Millipore). Following visualization, the blots were treated with stripping buffer (Restore, Pierce) for 5 min, reblocked with 5% nonfat dried milk for 60 min, and then incubated in the antibodies of GluN2B (1:1000; Millipore), CaMKII and GluR1 (1:1000; Cell Signaling Technology). Internal control was performed using a β-actin antibody (1:2000; Cell Signaling Technology). Western blot bands were scanned and analyzed with the image analysis software package (Image J; NIH Image, Bethesda, MD, USA).

2.9. Reverse transcription-polymerase chain reaction (RT-PCR)

Total RNA was extracted from the BLA with TRIzol reagent (Invitrogen, Camarillo, CA) following the manufacturer's protocol. Reverse transcriptions (RTs) were performed using a Prime Script RT reagent kit (Takara, China) for quantitative PCR (ABI Step One Plus, Foster City, CA) in the presence of a fluorescent dye (SYBR Green I; Takara, China). Expression levels of SERT (forward 5′-CTTCAGCCCCG GATGGTT-3′; reverse 5′-GTGGACTCATCAAAAAACTGCAAA-3′) were measured according to previous publication (Zajac et al., 2018). The results were normalized to GAPDH as reference genes using the 2-ΔΔct method.

2.10. Data analysis

Data are expressed as the means ± standard error (SE). Data were retrieved and processed with the software pCLAMP 10.0 (Molecular Devices, USA) and Micro cal Origin 9.2. All statistical analyses were performed using SPSS software, version 20.0 (SPSS Inc., USA). Two-group analysis was performed by Student's *t*-test (normally distributed data) or the Mann-Whitney-test (non-normally distributed data). For multiple comparison groups, analyses of variance (ANOVA) with the Bonferroni post hoc test were performed under homogeneity of variance. Repeated-measure ANOVA was used for input-output curve, paired-pulse inhibition, paired-pulse facilitation, LTP and LTD. The level of significance was set at $p < 0.05$.

3. Results

3.1. VCD-accelerated ovarian failure in mice induces anxiety-like behaviors

Twelve-week-old female mice were given intraperitoneal injections of VCD or vehicle for 20 consecutive days (Fig. 1A). At day 18 after the cessation of VCD, the ovarian histology revealed an obvious decrease in the numbers of primordial and primary follicles compared to control mice, with an increase in atretic primordial follicles (Fig. 1B). VCD-accelerated ovarian failure in mice (VCD-mice) caused a decline in the levels of serum E2 ($p = 0.036$, n = 10; Fig. 1C) and progesterone ($p = 0.006$, n = 10; Fig. 1D), which were not associated with the change in the basal level of corticosterone ($p > 0.05$, n = 10; Fig. 1E).

Open-field test (OFT) and elevated plus-maze test (EPM) performances, representing anxiety-like behaviors, were examined (n = 10 mice per experimental group). The total distance traveled observed in the OFT for VCD-mice did not differ significantly from control mice ($p > 0.05$; Fig. 1F). However, VCD-mice, compared to control mice, exhibited an obvious reduction in the time spent in the central portion of the arena ($p = 0.024$; Fig. 1F). Consistent with a recent report (Reis et al., 2014), the percentage of open arms entries during EPM in VCD-mice was less than that in control mice ($p = 0.018$; Fig. 1G). The administration of E2 from the day of the VCD cessation (Fig. 1A) could recover the time in the central portion of the arena in the OFT ($p = 0.005$) and the open arms entries in the EPM ($p = 0.040$), but it did not alter the affective behaviors in control mice ($p > 0.05$).

3.2. VCD reduces 5-HT synthesis to induces anxiety-like behaviors

The reduction of tryptophan hydroxylase (TPH)-positive cells in the entire DRN has been reported in VCD-treated rats (Pestana-Oliveira et al., 2018). Similarly, the immunoreactivity and number of TPH-positive cells in the DRN of VCD-mice were lower than those in the control DRN (Fig. 2A), which could be recovered by the treatment with E2. The level of serotonin reuptake transporter (SERT) expression in the BLA had no significant difference between VCD-mice and control mice ($p > 0.05$; Fig. 2B). The level of *SERT* mRNA in the BLA of VCD-mice failed to be altered by the administration of E2 ($p > 0.05$). To test whether the decline in 5-HT synthesis in VCD-mice was associated with their anxiety-related behaviors, the VCD-mice ($n = 10$ mice per experimental group) were treated with the administration of the 5-HT1Ar agonist 8-OH-DPAT, the 5-HT1Br agonist CGS, the 5-HT2A/Cr agonist DOI for 2 days (Fig. 2C). The results showed that the co-administration with 8-OH-DPAT and DOI in VCD-mice could recover the time spent in the central portion of the arena in the OFT ($p = 0.004$; Fig. 2D) and open arms entries in the EPM ($p = 0.009$; Fig. 2E), but the administration of alone 8-OH-DPAT ($p > 0.05$), CGS ($p > 0.05$), DOI ($p > 0.05$) or the co-administration of 8-OH-DPAT and CGS ($p > 0.05$) did not display an effective operation. These results indicate that the down-regulation of 5-HT1Ar and 5-HT2A/Cr may be responsible for anxiety-like behaviors in VCD-mice.

3.3. EC-BLA synaptic transmission in VCD-mice

To explore the mechanisms underlying anxiety-like behaviors induced by VCD-accelerated ovarian failure, we examined the basal synaptic properties in the BLA using a field potential recording ($n = 6$ slices/6 mice per experimental group). First, the excitatory postsynaptic potential (EPSP) in the BLA was evoked by stimulating external capsule (EC) fibers (Fig. 3A). The EC-BLA synaptic transmission was blocked by the application of AMPAr antagonist CNQX but not by the NMDAr antagonist AP-V (Fig. 3B-i). The application of the $GABA_AR$ antagonist bicuculline caused an increase in duration of EPSP but failed to significantly alter the EPSP slope (Fig. 3B-ii). The input-output curve was built by plotting the EPSP slopes against stimulation intensities (SI) from 0.1 mA to 0.8 mA. As shown in Fig. 3C, the EPSP slopes were progressively increased with enhancing stimulus intensities in the both groups ($F_{(7,70)} = 87.853$, $p < 0.001$) and was affected by the VCD treatment ($F_{(1,10)} = 9.030$, $p = 0.013$). In comparison with control mice, the EPSP slopes evoked by 0.4–0.7 mA stimulus intensities were larger in VCD-mice than those in control mice (0.4 mA, $p = 0.005$; 0.5 mA, $p = 0.006$; 0.6 mA, $p = 0.020$; 0.7 mA: $p = 0.031$).

To further evaluate the $GABA_AR$-mediated inhibitory circuit and the capability of presynaptic glutamate release, the paired-pulse inhibition (PPI) and paired-pulse facilitation (PPF) of EPSP slopes were examined by delivering paired-pulse stimulation (0.5-mA SI) with 20–30 ms and 50–100 ms interpulse intervals (IPIs), respectively. There was a main effect of VCD treatment for the PPF value ($F_{(1,10)} = 7.108$, $p = 0.024$; Fig. 3D) rather than the PPI value ($F_{(1,10)} = 1.487$, $p = 0.251$). In comparison with controls, the PPF value was remarkably reduced in VCD-mice (50 ms, $p = 0.038$; 75 ms, $p = 0.033$; 100 ms, $p = 0.045$). Although the VCD-mice had a tendency of an increase in the PPI value, this failed to reach significance when compared to controls ($p > 0.05$). In VCD-mice treated with E2 (Fig. 1), the EPSP slopes (0.5 mA SI, $p > 0.05$; Fig. 3E), the PPF value (50 ms IPI, $p > 0.05$; Fig. 3F) or the PPI value (20 ms IPI, $p > 0.05$; Fig. 3G) did not differ significantly from control mice. The administration of E2 to control mice did not alter the EPSP slopes ($p > 0.05$) or the values of PPF ($p > 0.05$) and PPI ($p > 0.05$). These results indicate that the presynaptic glutamate release in the BLA of VCD-mice is enhanced.

3.4. Effects of 5-HTs agonists on EC-BLA synaptic transmission in VCD-mice

The 5-HT level in amygdala of VCD-treated rats has been reported to be lower than that in control rats (Pestana-Oliveira et al., 2018). As shown in Fig. 4A, the immunoreactivity and density of TPH+ fibers in the BLA of VCD-mice were significantly reduced compared to control mice, reflecting a reduced 5-HT afferent to the BLA. Sequentially, the slices obtained from VCD-mice (VCD-slices) and control mice (control slices) were treated with acute (2–3 min) perfusion of the 5-HT1Ar agonist 8-OH-DPAT, the 5-HT1Br agonist CGS, the 5-HT2A/Cr agonist DOI or the 5-HT1Ar antagonist WAY-100635 or the 5-HT2r antagonist sarpogrelate ($n = 6$ slices/6 mice per experimental group). In control slices, the perfusion of 8-OH-DPAT caused a decrease in EPSP slopes ($p = 0.012$; Fig. 4B) with an increase in the PPF value ($p = 0.036$; Fig. 4C); the perfusion of WAY-100635 remarkably increased the EPSP slopes ($p = 0.026$) with a decrease in the PPF value ($p = 0.022$). In VCD-slices, the application of 8-OH-DPAT reduced the EPSP slopes ($p = 0.002$) and increased the PPF value ($p = 0.003$). In the presence of 8-OH-DPAT, the EPSP slopes and the PPF value had no significant difference between VCD-slices and control slices ($p > 0.05$). In contrast, the application of CGS ($p > 0.05$) or DOI ($p > 0.05$) in control slices or VCD-slices had no significant effect on the EC-BLA synaptic transmission.

The perfusion of 8-OH-DPAT in control slices did not alter the PPI value ($p > 0.05$; Fig. 4D). Interestingly, the perfusion of 8-OH-DPAT in VCD-slices caused an increase in the PPI value ($p = 0.022$), which could be corrected by the addition of DOI ($p = 0.002$) rather than CGS ($p > 0.05$). In control slices, the perfusion of sarpogrelate could increase the PPI value ($p = 0.004$). The perfusion of DOI alone did not alter the PPI value in control slices or VCD-slices ($p > 0.05$). These results indicate that in VCD-mice the down-regulation of 5-HT1Ar increases glutamate release, which masks the dysfunction of GABAergic feedback inhibition; the down-regulation of 5-HT2r weakens GABAergic feedback inhibition.

3.5. Induction of synaptic plasticity in the BLA of VCD-mice

The alteration of glutamatergic or GABAergic transmission in the BLA can affect the induction of synaptic plasticity (Zhang et al., 2017). We further examined the induction of LTP and LTD in the BLA ($n = 6$

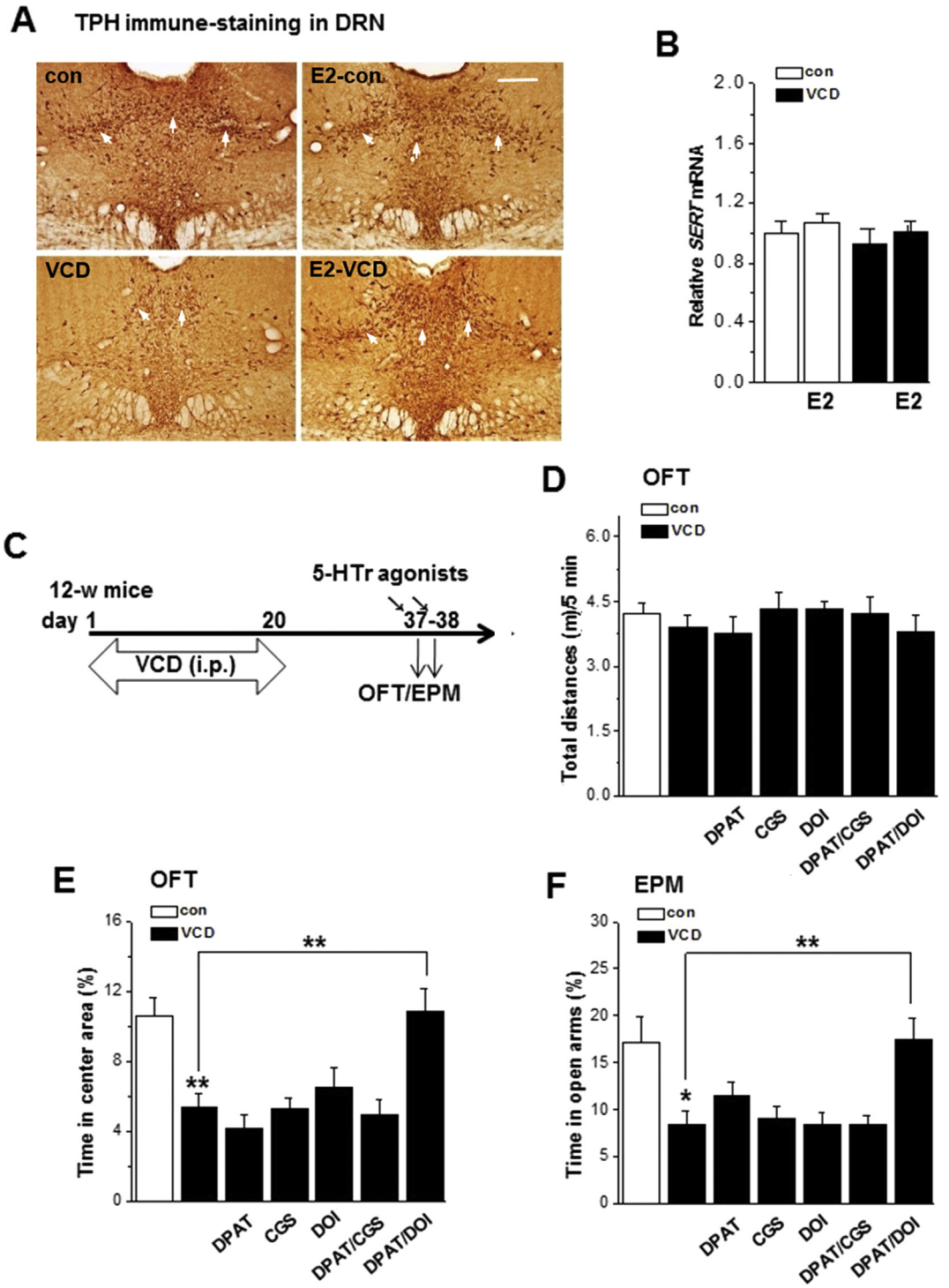

Fig. 2. VCD reduces 5-HT synthesis to induces anxiety-like behaviors. (A) Representative images of immune-staining for tryptophan hydroxylase (TPH) in mid DRN of control mice and VCD-mice treated with E2. Scale bars = 200 μm. Arrows indicate TPH positive cells. (B) Bars show the levels of *SERT* mRNA in control mice and VCD-mice treated with E2. (C) Experimental timeline. Horizontal arrow indicates the time (day) of VCD injection. ↘: time of 5-HTr agonists administrated after stopping VCD. (D&E) Bars show the distance traveled (m) and the time spent in the central portion (%) during the OFT in VCD-mice treated with 5-HT1Ar agonist 8-OH-DPAT (DPAT), 5-HT1Br agonist CGS, 5-HT2r agonist DOI. $^{**}p < 0.01$ (one-way ANOVA). (F) Bar graph shows the time spent in the open arms of EPM (%).$^{*}p < 0.05$ and $^{**}p < 0.01$ (one-way ANOVA).

slices/6 mice per experimental group). The five trains high-frequency stimulation (HFS × 5) induced an increase in the EPSP slopes for over 60 min in control mice (Fig. 5A), indicative of LTP induction. The same protocol was able to induce a stable LTP in the VCD-mice. Interestingly, one train sub-threshold HFS (HFS × 1) could induce the production of LTP in VCD-mice rather than in control mice ($F_{(1,10)} = 6.643$, $p = 0.028$; Fig. 5B), indicative of "LTP facilitation". Either the HFS × 5-induced LTP in control mice or the induction of LTP by HFS × 1 in VCD-mice depended on the activation of NMDAr (Fig. 5C). In E2-treaed VCD-mice or E2-treaed control mice, the HFS × 1 protocol failed to induce LTP (Fig. 5D).

The application of low frequency stimulation (LFS) in control mice

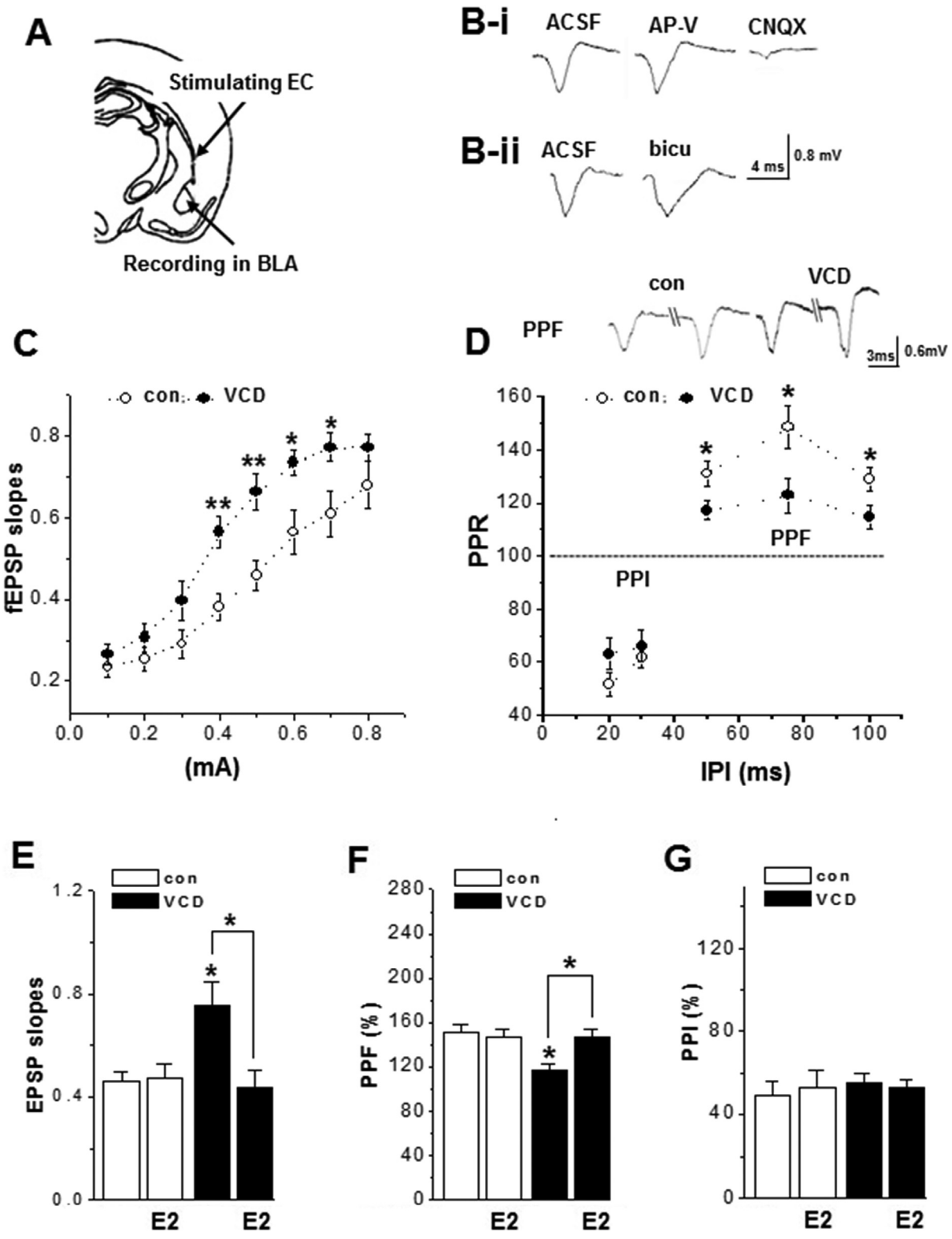

Fig. 3. EC-BLA synaptic transmission in VCD-mice. (A) Field potential recordings were carried out from the BLA in acute brain slices. By stimulating external capsule (EC) fibers, field excitatory post-synaptic potentials (EPSPs) were recorded in the BLA. (B) Representative traces of EPSP evoked by 0.5 mA stimulation intensities (SI) in control slices treated with 3 min perfusion of AMPAr antagonist CNQX, NMDAr antagonist AP-V, or $GABA_AR$ antagonist bicuculine (bicu). (C) Input/output curve. EPSP slopes were plotted against stimuli ranging from 0.1 mA to 0.8 mA in control slices and VCD-slices. Typical traces evoked by 0.5 mA SI. $*p < 0.05$ and $**p < 0.01$ (repeated-measure ANOVA). (D) Paired-pulse inhibition (PPI) and facilitation (PPF) of EPSPs. Paired pulse ratios (PPR, %) of EPSP slopes were plotted against inter-pulse intervals (IPI) of 20–30 ms (PPI) and 50–100 ms (PPF). $*p < 0.05$ (repeated-measure ANOVA). (*E*-G) Bar graphs show the EPSP slopes and the values of PPF and PPI in control mice and VCD-mice treated with E2. $*p < 0.05$ (two-way ANOVA).

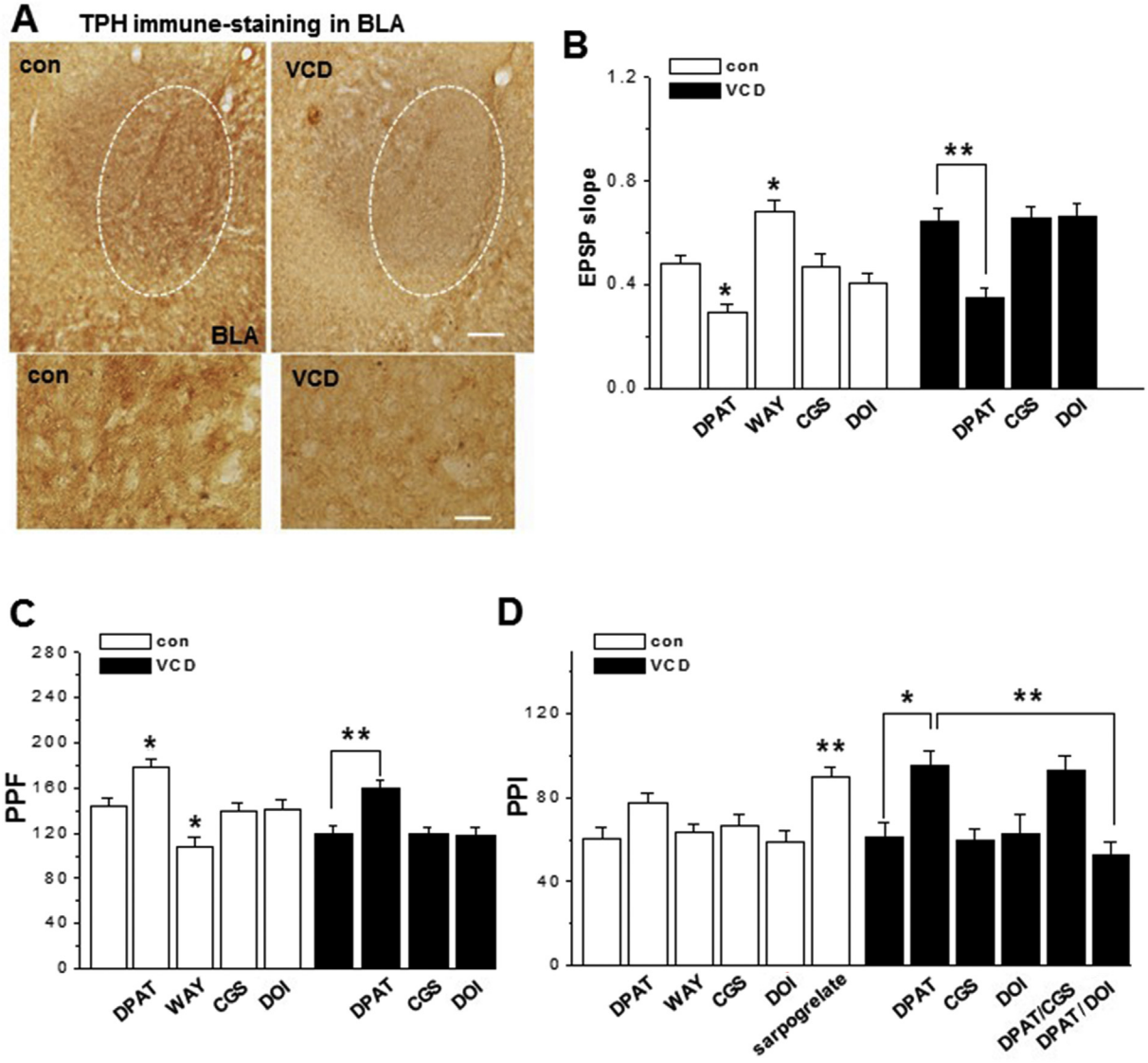

Fig. 4. VCD-reduced 5-HT1R activity enhances presynaptic glutamate release. (A) Representative images of immune-staining for TPH in BLA (ring of point lines). Scale bars = 100 μm (upper). Higher-power views in bottom-right inset. Scale bars = 25 μm. Arrows indicate TPH positive fibers. (B–D) The values of EPSP slopes, PPF and PPI in control slices or VCD-slices treated with bath-application of 8-OH-DPAT (DPAT), WAY-100635(WAY), CGS, DOI or sarpogrelate for 5 min. *$p < 0.05$ and **$p < 0.01$ (two-way ANOVA).

induced approximately 40% decline in the EPSP slopes lasting 60 min (Fig. 5E), indicative of LTD induction. However, the same LFS protocol could not induce a stable LTD in VCD-slices ($F_{(1,10)} = 13.471$, $p = 0.004$), indicative of "LTD impairment". The NMDAr-independent LTD in control mice was blocked by the application of bicuculine ($F_{(1,10)} = 8.647$, $p = 0.015$; Fig. 5F). The administration of E2 could recover the induction of LTD in VCD-mice (Fig. 5G), whereas it did not affect the induction of LTD in control mice.

3.6. Effects of 5-HTr agonists on synaptic plasticity in VCD-mice

Next experiments were designed to determine whether the down-regulation of 5-HT1Ar and 5-HT2A/Cr was involved in the LTP facilitation and LTD impairment of VCD-mice (n = 6 slices/6 mice per experimental group). The perfusion of 8-OH-DPAT in VCD-slices could prevent the facilitation of LTP (Fig. 6A), whereas the application of CGS or DOI did not (Fig. 6B). The perfusion of WAY-100635 could cause the facilitation of LTP in control slices ($F_{(1,10)} = 6.531$, $p = 0.029$; Fig. 6A). These results indicate that the increased presynaptic glutamate release by the down-regulation of 5-HT1Ar in VCD-mice facilitates NMDAr-dependent LTP induction. (See Fig. 7).

In VCD-slices, the LTD impairment was rescued by the co-application of 8-OH-DPAT and DOI ($F_{(1,10)} = 6.471$, $p = 0.029$; Fig. 6C), but not the perfusion of 8-OH-DPAT, CGS or DOI alone (Fig. 6D), or the co-application of 8-OH-DPAT and CGS (Fig. 6E). Notably, the application of sarpogrelate abolished the LTD induction in control mice. The application of muscimol in VCD-slices had no effect on the impairment of LTD (Fig. 6F), whereas the co-application of muscimol and 8-OH-DPAT could recover the induction of LTD ($F_{(1,10)} = 18.072$, $p = 0.002$). These results indicate that increased presynaptic glutamate release or reduced GABAergic inhibition in VCD-mice can impair the NMDAr-independent LTD induction.

3.7. AMPAr, NMDAr and $GABA_AR$ expression and activities in the BLA of VCD-mice

To explore the mechanisms underlying increased EC-BLA synaptic transmission, reduced GABAergic inhibition, facilitation of LTP and impairment of LTD in VCD-mice, we further examined the expression and phosphorylation of AMPAr, NMDAr and $GABA_AR$ (3 slices/mice,

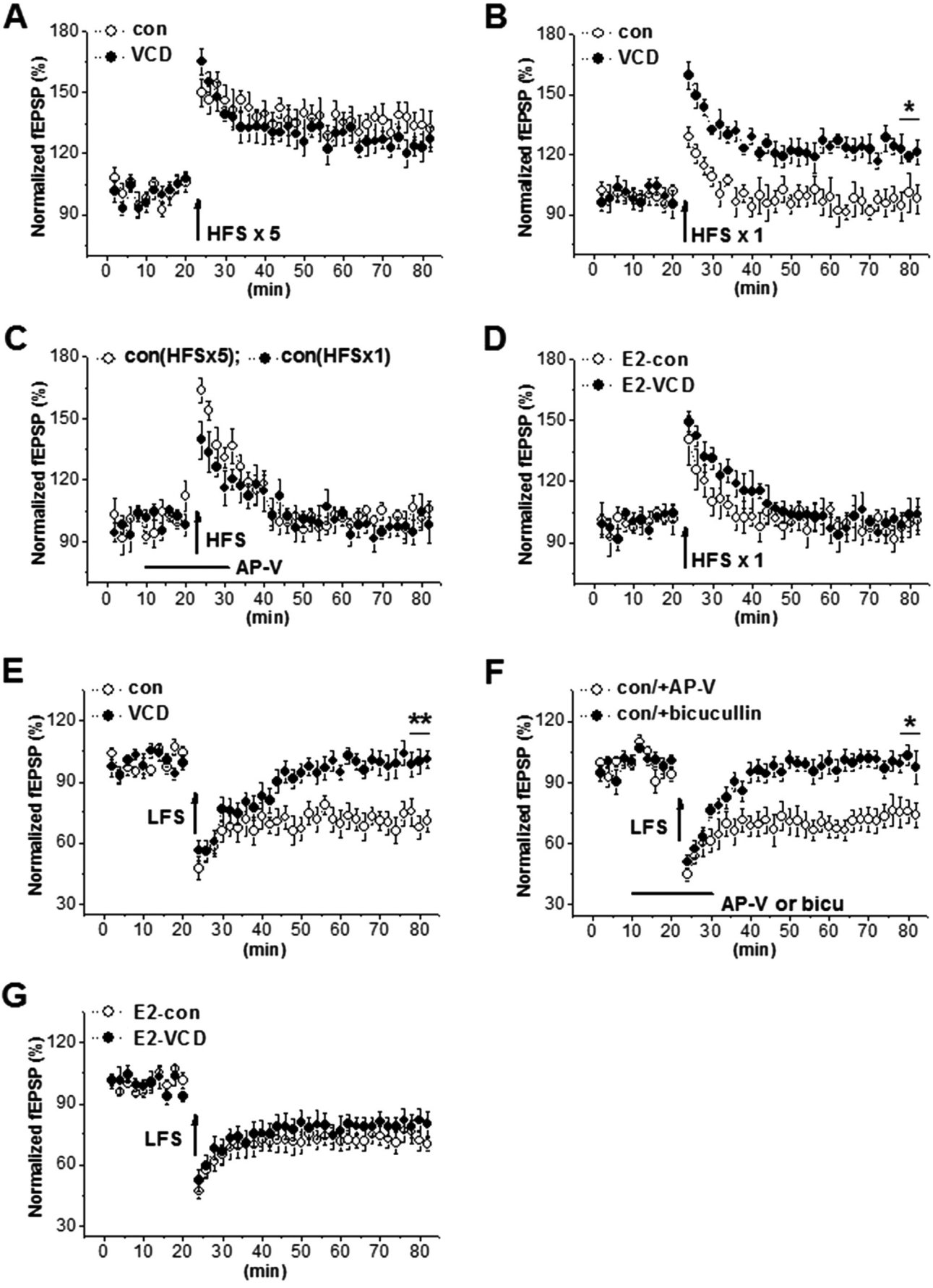

(caption on next page)

Fig. 5. VCD-mice show LTP facilitation and LTD impairment. (A&B) Induction of LTP by HFS (HFS × 5 or HFS × 1) in control slices and VCD-slices. Each point represents the mean value (± SEM) of EPSP slopes expressed as percentage of baseline. A solid arrow indicates when HFS was given. *$p < 0.05$ (repeated-measure ANOVA). (C) Induction of LTP by HFS × 5 in control slices or HFS × 1 in VCD-slices in the presence of AP-V. Black line indicates duration of AP-V applied. (D) Induction of LTP by HFS × 1 in control mice and VCD-mice treated with E2. (E) Induction of LTD by LFS (1 Hz for 15 min) in control slices and VCD-slices. **$p < 0.01$ (repeated-measure ANOVA). (F) Induction of LTD by LFS in control slices treated with AP-V or bicuculine (bicu). *$p < 0.05$ (repeated-measure ANOVA). Black line indicates duration of AP-V and bicuculine applied. (G) Induction of LTD in control mice and VCD-mice treated with E2.

$n = 5$ mice per experimental group). RT-PCR analysis showed that the levels of GluR1, GluR2, NR1, NR2B, $GABA_AR$-a4 and $GABA_AR$-d mRNA in the BLA had no significant difference between VCD-mice and control mice ($p > 0.05$; Fig. 6A).

The expression levels of AMPAr GluR1 (Fig. 6B), NMDAr NR2B (Fig. 6C), and CaMKII (Fig. 6D) or the basal levels of GluR1 phosphorylation (phosphor-GluR1, $p > 0.05$), NR2B phosphorylation (phosphor-NR2B, $p > 0.05$), and CaMKII phosphorylation (phosphor-CaMKII, $p > 0.05$) in VCD-mice did not differ from WT mice. At 10 min after HFS × 1, the levels of phosphor-CaMKII ($p = 0.002$) in VCD-mice were higher than that in control mice, which were sensitive to the application of the NMDAr channel blocker MK801 ($p = 0.006$) or 8-OH-

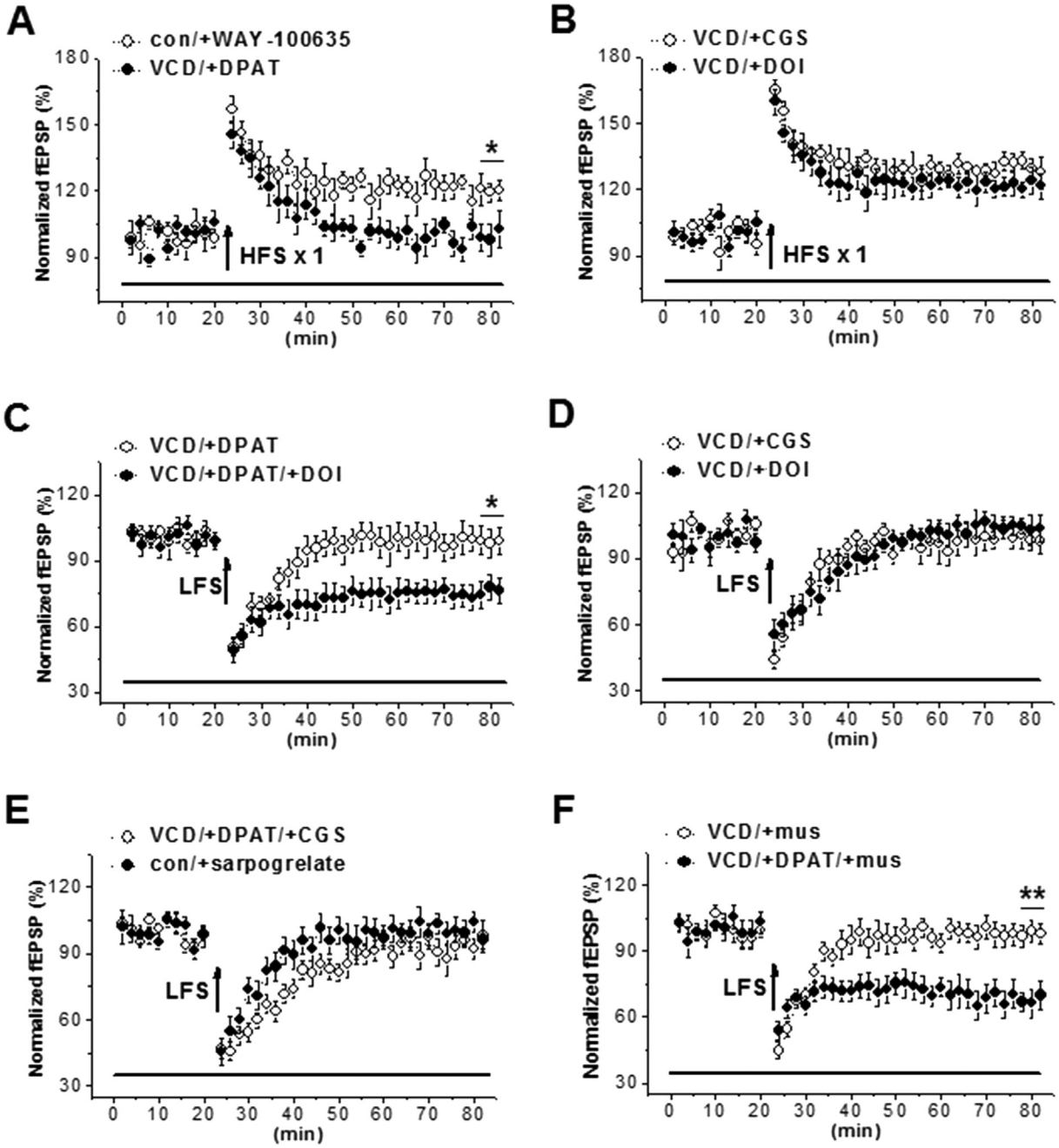

Fig. 6. VCD-reduced 5-HT causes LTP facilitation and LTD impairment. (A&B) Induction of LTP by HFS × 1 in control slices treated with WAY-100635 or in VCD-slices treated with 8-OH-DPAT, CGS, DOI. *$p < 0.05$ (repeated-measure ANOVA). (C–F) Induction of LTD in control slices treated with sarpogrelate or in VCD-slices treated with bath-application of 8-OH-DPAT, CGS, DOI or muscimol. Black line indicates duration of the drugs applied. *$p < 0.05$ and **$p < 0.01$ (repeated-measure ANOVA).

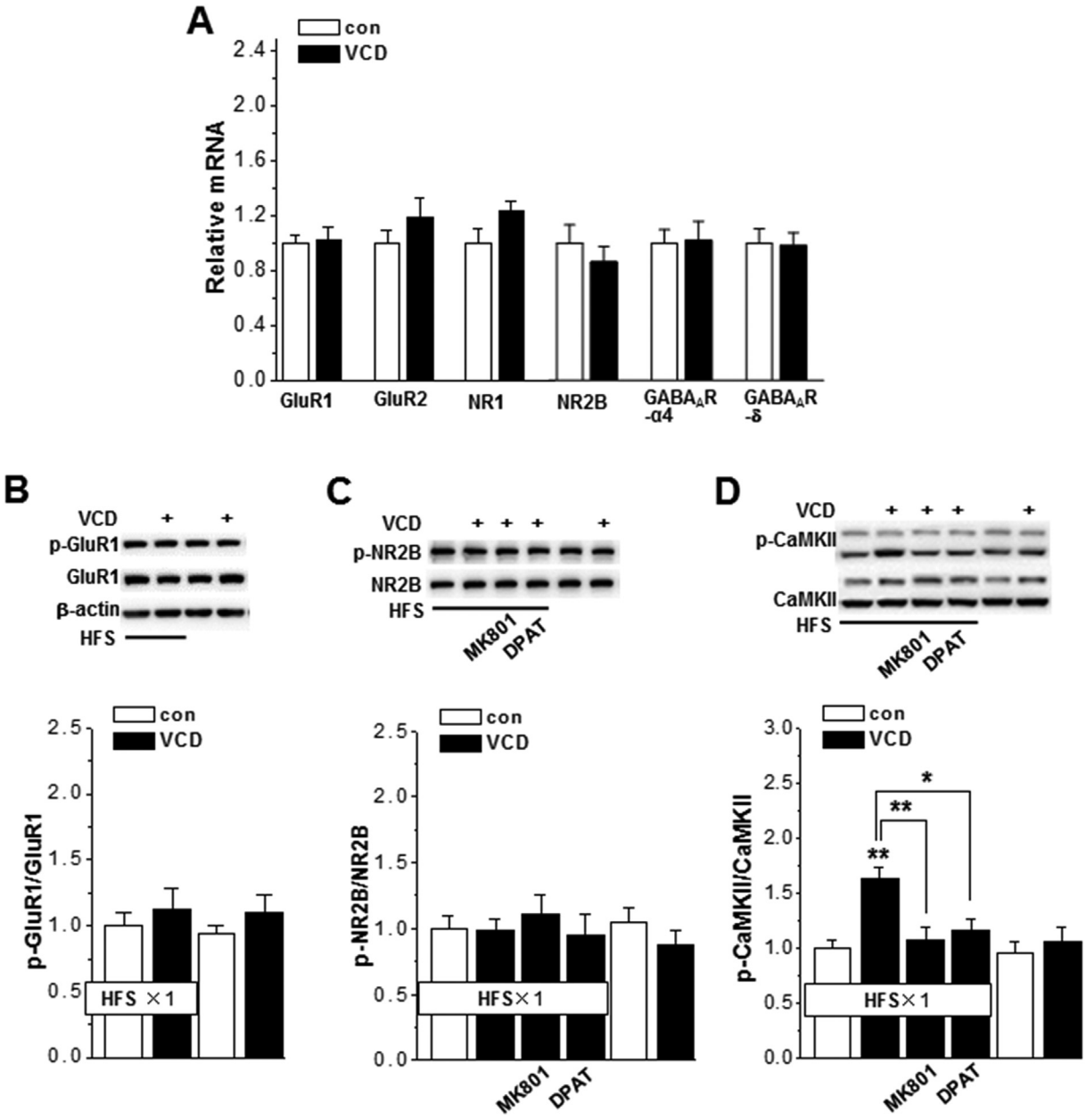

Fig. 7. VCD-reduced 5-HT increases CaMKII phosphorylation after HFS × 1. (A) Levels of *GluR1*, *GluR2*, *NR1*, *NR2B*, *GABA$_A$R-α4* and *GABA$_A$R-δ* mRNA in BLA of VCD-mice and control mice. (B-D) Levels of basal and after HFS (10 min after HFS × 1) of phosphor-GluR1, phosphor-NR2B and phosphor-CaMKII in control slices or VCD-slices treated with MK801, 8-OH-DPAT. *$p < 0.05$ and **$p < 0.01$ (one-way ANOVA).

DPAT ($p = 0.023$). In contrast, the levels of phosphor-GluR1 ($p > 0.05$) or phosphor-NR2B ($p > 0.05$) after HFS × 1 had no significant difference between VCD-mice and control mice.

4. Discussion

The present study determined that VCD-accelerated ovarian failure in mice caused anxiety-like behaviors with the decline in serum E2 and progesterone. During human menopause, E2 levels are very low or undetectable, progesterone levels decrease (Nejat and Chervenak, 2010). In contrast, the E2 plasma concentrations remain unchanged in female rats treated with VCD (VCD-rats) for 15 days (Pestana-Oliveira et al., 2018; Reis et al., 2014). In this study, mice were injected with VCD for 20 days. Thus, this contradictory of E2 levels between VCD-mice and VCD-rats may arise from the difference in the experimental protocol or the animal species. When B6C3F1 female mice are treated with VCD for 10 consecutive days, the decline of E2 level occurs by approximately day 110 after the onset of VCD administration (Brooks et al., 2016). However, when mice are treated with VCD for 20 consecutive days, the onset of E2 decline can be accelerated to day 44. In addition, as aging progresses to about 16–18 months, mice appeared the persistent estrus with decline of E2 levels (Rousseau, 2006), but rats did not (Maffucci and Gore, 2006). The mice had complete follicular exhaustion at 24 months of age and a greater decrease in E2 levels, whereas rats retained a larger number of primary follicles and the E2 levels (Maffucci and Gore, 2006).

The VCD-mice showed an obvious decrease in the 5-HT synthesis in the DRN, which was recovered by the supplement E2. Estradiol treatment in VCD-treated rats has been reported to restore the synthesis of 5-HT (Pestana-Oliveira et al., 2018). Consistent with our results, the supplement E2 in VCD-treated rats can not only recover the expression of 5-HT in the DRN but not decrease their anxiety-like behaviors (Hiroi

et al., 2006). Estradiol therapy in perimenopause and postmenopause women reverses the decreased serotonergic activity (Halbreich et al., 1995) and improves the affective disorder (Gleason et al., 2015). The estrogen treatment in spayed monkeys increased the level of TPH expression (Bethea et al., 2000). TPH knockdown reduced the anxiolytic effects of E2 (Hiroi and Neumaier, 2011). The activation of estrogen receptor β (ERβ) is required for regulation of serotonin synthesis (Hiroi et al., 2006) and can decrease serotonin degradation by inhibiting monoamino-oxidase activity (Gundlah et al., 2005). The ERβ mutant in female mice caused anxiety-like behaviors (Krezel et al., 2001). Early data indicated that the estradiol treatment increased the density of serotonin reuptake sites (Bethea et al., 2002); the density of SERT was reduced in ovariectomized mice (Bertrand et al., 2005). The application of estradiol increased SERT activity through the activation of nuclear estrogen receptors (Kranz et al., 2015). SERT proteins are down-regulated when 5-HT levels are low. However, the level of SERT expression in the BLA of VCD-mice did not differ significantly from control mice. 5-HT1Ar knockout mice exhibit increased anxiety-like behaviors (Klemenhagen et al., 2006). The anxiety-like behaviors in VCD-mice were relieved by the co-administration of 5-HT1Ar and 5-HT2A/Cr agonists, indicating that the 5-HT deficiency in VCD-mice is responsible for their anxiety-like behaviors.

The decline of TPH positive fibers in the BLA of VCD-mice reflects a decreased 5-HT afferent from DRN to BLA. An earlier study reported that 5-HT potently suppresses excitatory synaptic transmission *via* 5-HT1Ar-mediated inhibition of presynaptic glutamate release (Schmitz et al., 1998). Activation of 5-HT1Ar hyperpolarizes neurons by a pertussistoxin-sensitive G-protein and the opening of a Ca^{2+} independent K^+ channel (Penington et al., 1993). Indeed, the probability of presynaptic glutamate release at the EC-BLA synaptic transmission was enhanced in VCD-mice, which was corrected by the 5-HT1Ar agonist or the estrogen treatment, but not the 5-HT1Br agonist or the 5-HT2A/Cr agonist. The blockade of 5-HT1Ar caused an increase in probability of presynaptic glutamate release in control mice. Thus, one simple explanation is that the deficiency of 5-HT in VCD-mice enhances presynaptic glutamate release *via* down-regulation of 5-HT1Ar.

The induction of LTP in the BLA principal neurons is well known to be a cell model of the fear memory acquisition (Goosens and Maren, 2002). A principal observation in VCD-mice is the facilitation of NMDAr-dependent LTP. The activation of 5-HT1Ar could prevent the facilitation of LTP in VCD-mice, while the blockade of 5-HT1Ar in control mice was able to reduce the threshold of LTP induction. The induction of NMDAr-dependent LTP is modulated probably by the presynaptic transmitter release or postsynaptic NMDAr Ca^{2+} influx. Thus, one possible explanation is that the increased glutamate release by the down-regulation of 5-HT1Ar can promote the NMDAr-dependent LTP induction. On the other hand, the activation of postsynaptic 5-HT1Ar has also been shown to suppress NMDAr-dependent LTP in the hippocampus (Sakai and Tanaka, 1993) and in the visual cortex (Edagawa et al., 1999). A microdialysis study demonstrated an interaction between 5-HT1Ar and NMDAr. Activation of 5-HT1Ar reduces Ca^{2+} influx through NMDAr channels (Yuen et al., 2008) through a reduction in surface expression of NMDAr NR2B subunit (Yuen et al., 2005). Activation of 5-HT1Ar also reduced CaMKII activity and the AMPAr GluR1 subunit phosphorylation as well as surface expression of the GluR2/3 subunits (Cai et al., 2002; Schiapparelli et al., 2005). Although the levels of NR2B or GluR1 subunit phosphorylation before and after HFS × 1 in the BLA of VCD-mice were unchanged compared to controls, the level of CaMKII phosphorylation after HFS × 1 was elevated significantly. The increased CaMKII phosphorylation and the facilitation of LTP in the BLA of VCD-mice were sensitive to the NMDAr channel blocker or the 5-HT1Ar agonist. Therefore, another possible explanation is that the down-regulation of 5-HT1Ar increases the Ca^{2+} influx of NMDAr during HFS.

The activation of 5-HT2r directly activates GABAergic interneurons of the BLA and increases the frequency of inhibitory synaptic events in projection neurons (Rainnie, 1999). The blockade of $GABA_AR$ attenuated the local feedback GABAergic inhibition at the EC-BLA synaptic transmission (Zhang et al., 2017). Interestingly, the feedback GABAergic inhibition in VCD-mice did not differ significantly from control mice, whereas in the presence of the 5-HT1Ar agonist it was decreased compared to control mice, which was corrected by the activation of 5-HT2A/Cr. In addition, the blockade of 5-HT2A/Cr attenuated the GABAergic inhibition in control mice. The application of the 5-HT1Ar agonist to the hippocampal dentate gyrus reduced somatic GABAergic inhibition (Sanberg et al., 2006). The 5-HT1Ar knockout mice displayed a decline of the $GABA_AR$ α1 and α2 subunits in the amygdala (Pattij et al., 2002). However, the level of $GABA_AR$ expression in the BLA of VCD-mice was unchanged. Thus, it is proposed that the down-regulation of 5-HT1Ar in VCD-mice enhances feedforward excitatory input onto interneurons, which can mask the decline in 5-HT2A/Cr-mediated GABAergic inhibition.

A critical finding in VCD-mice is the impairment of NMDAr-independent LTD. A wide body of evidence suggests that the GABAergic inhibition in the mouse BLA is pivotal for the LTD induction (Bissiere et al., 2003), because blocked GABAergic synaptic transmission prevents the production of LTD (Rammes et al., 2001). The deficit in GABAergic inhibition in amygdala is a critical cellular mechanism in the development of anxiety (Wu et al., 2008). An earlier study reported that 5-HT1Ar activation promoted the induction of LTD (Garraway and Hochman, 2001). The serotonergic projection on inhibitory interneurons has been reported to alter synaptic plasticity *via* silencing GABAergic inhibition (Sanberg et al., 2006). Interestingly, the activation of 5-HT1Ar was required for the $GABA_AR$ agonist or 5-HT2A/Cr agonist-rescued LTD induction in VCD-mice. Thus, it is indicated that the enhancemnt of postsynaptic excitability or the facilitation of LTP in VCD-mice might be involved in the LTD impairment, in addition to the dysfunction of GABAergic inhibition. The impairment of LTD in the BLA has been associated with the deficit in extinction of a fear memory (Kim et al., 2007) or the production of anxiety-related behaviors (Yang et al., 2017; Zhang et al., 2017). The impaired performance in anxiety-related tasks is thought to be due to an enhanced fear response in aversive environments (Gross et al., 2000). The co-activation of 5-HT1Ar and 5-HT2A/Cr or the estrogen treatment in VCD-mice could recover LTD induction and relieve anxiety-like behaviors. Based on the data, the following model is proposed: the deficiency of 5-HT in the BLA of VCD-mice *via* down-regulation of 5-HT1Ar and 5-HT2A/Cr causes dysfunction of GABAergic inhibition, excitability of postsynaptic neurons or LTP facilitation, which impairs LTD induction leading to anxiety-like behaviors (Fig. 8).

The perimenopause is associated with the occurrence of depression, which is also tied to the serotonergic system. The impairment of LTD induction in the BLA has been reported to cause the production of depressive-like behaviors (Zhang et al., 2017). Indeed, we observed the depression-like behaviors in VCD-mice, showing the longer immobility during forced swim test (FST) and tail suspension test (TST) than those in control mice (Supplementary data: S-Fig. 1). However, the co-administration with 8-OH-DPAT and DOI in VCD-mice failed to recover the immobility during FST and TST. In addition, BLA receives dense dopaminergic innervations from the ventral tegmental area (VTA). Dopamine and dopaminergic receptors play a significant role in neuroplasticity and modulation of neural activity in the BLA. Stimulatory D1-like receptors (D1R) can attenuate firing of BLA projection neurons and activation of BLA interneurons (Pape, 2005; Rosenkranz and Grace, 1999). By contrast, the number of tyrosine hydroxylase-positive (TH +) cells or TH immunoreactivity in the midbrain ventral tegmental area (VTA) or substantia nigra (SNpc) of VCD-mice did not differ significantly from control mice (data not shown). Although VCD-mice exhibited a reduction in the time spent in the central portion of the arena during the OFT, the total distance traveled was unchanged compared to control mice. Therefore, further experiments should be done to clarify the mechanims underlying the VCD-induced depressive-

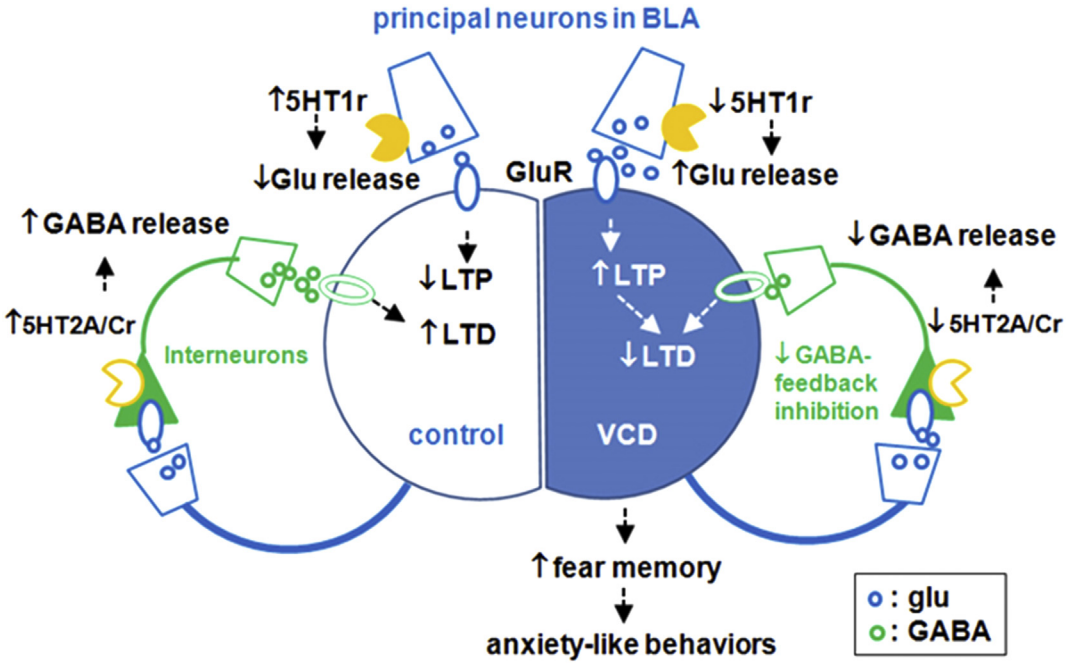

Fig. 8. The hypothesis of molecular mechanisms underlying VCD-reduced 5-HT to induce anxiety-related behaviors. VCD-reduced 5-HT afferents to BLA impairs LTD induction through LTP facilitation and dysfunction of GABAergic inhibition, leading to anxiety-like behaviors. ↑: increase; ↓: decrease.

like behaviors.

5. Conclusions

Through the model of perimenopause mice by VCD-accelerated natural follicular depletion, the present study demonstrated that the deficiency of 5-HT through the down-regulation of 5-HT1Ar and 5-HT2A/Cr in the BLA is responsible for anxiety-like behaviors. The results indicate that estradiol therapy ameliorates perimenopause and postmenopause anxiety probably by boosting the serotonin pathway.

Contributors

Wang Y. performed the electrophysiological experiments and all statistical analysis. Liu J. undertook the western blot analysis. Xiong J. carried out the animal care and the behavioral examinations. Chen L. and Wu J. carried out the experimental design and the preparation of the manuscript.

Declaration of Competing Interest

The authors declare that they have no conflict of interest.

Acknowledgments

This work was supported by National Natural Science Foundation of China (81671253; 81471157), Jiangsu provincial Natural Science Foundation (BE2016765).

Appendix A. Supplementary data

Supplementary data to this article can be found online at https://doi.org/10.1016/j.expneurol.2019.113030.

References

Bertrand, P.P., Paranavitane, U.T., Chavez, C., Gogos, A., Jones, M., van den Buuse, M., 2005. The effect of low estrogen state on serotonin transporter function in mouse hippocampus: a behavioral and electrochemical study. Brain Res. 1064, 10–20.

Bethea, C.L., Gundlah, C., Mirkes, S.J., 2000. Ovarian steroid action in the serotonin neural system of macaques. Novartis Found. Symp. 230, 112–130 (discussion 130-113).

Bethea, C.L., Mirkes, S.J., Su, A., Michelson, D., 2002. Effects of oral estrogen, raloxifene and arzoxifene on gene expression in serotonin neurons of macaques. Psychoneuroendocrinology 27, 431–445.

Bissiere, S., Humeau, Y., Luthi, A., 2003. Dopamine gates LTP induction in lateral amygdala by suppressing feedforward inhibition. Nat. Neurosci. 6, 587–592.

Bobker, D.H., Williams, J.T., 1989. Serotonin agonists inhibit synaptic potentials in the rat locus ceruleus in vitro via 5-hydroxytryptamine1A and 5-hydroxytryptamine1B receptors. J. Pharmacol. Exp. Ther. 250, 37–43.

Brooks, H.L., Pollow, D.P., Hoyer, P.B., 2016. The VCD mouse model of menopause and perimenopause for the study of sex differences in cardiovascular disease and the metabolic syndrome. Physiology 31, 250–257.

Bryant, C., Judd, F.K., Hickey, M., 2012. Anxiety during the menopausal transition: a systematic review. J. Affect. Disord. 139, 141–148.

Burger, H.G., Dudley, E.C., Hopper, J.L., Shelley, J.M., Green, A., Smith, A., Dennerstein, L., Morse, C., 1995. The endocrinology of the menopausal transition: a cross-sectional study of a population-based sample. J. Clin. Endocrinol. Metab. 80, 3537–3545.

Cai, X., Gu, Z., Zhong, P., Ren, Y., Yan, Z., 2002. Serotonin 5-HT1A receptors regulate AMPA receptor channels through inhibiting Ca2+/calmodulin-dependent kinase II in prefrontal cortical pyramidal neurons. J. Biol. Chem. 277, 36553–36562.

Chen, T., Zhang, B., Li, G., Chen, L., Chen, L., 2016. Simvastatin enhances NMDA receptor GluN2B expression and phosphorylation of GluN2B and GluN2A through increased histone acetylation and Src signaling in hippocampal CA1 neurons. Neuropharmacology 107, 411–421.

Deecher, D., Andree, T.H., Sloan, D., Schechter, L.E., 2008. From menarche to menopause: exploring the underlying biology of depression in women experiencing hormonal changes. Psychoneuroendocrinology 33, 3–17.

Dere, E., De Souza-Silva, M.A., Spieler, R.E., Lin, J.S., Ohtsu, H., Haas, H.L., Huston, J.P., 2004. Changes in motoric, exploratory and emotional behaviours and neuronal acetylcholine content and 5-HT turnover in histidine decarboxylase-KO mice. Eur. J. Neurosci. 20, 1051–1058.

Edagawa, Y., Saito, H., Abe, K., 1999. Stimulation of the 5-HT1A receptor selectively suppresses NMDA receptor-mediated synaptic excitation in the rat visual cortex. Brain Res. 827, 225–228.

Ehrlich, I., Humeau, Y., Grenier, F., Ciocchi, S., Herry, C., Luthi, A., 2009. Amygdala inhibitory circuits and the control of fear memory. Neuron 62, 757–771.

File, S.E., Gonzalez, L.E., Gallant, R., 1998. Role of the basolateral nucleus of the amygdala in the formation of a phobia. Neuropsychopharmacology 19, 397–405.

Garraway, S.M., Hochman, S., 2001. Serotonin increases the incidence of primary afferent-evoked long-term depression in rat deep dorsal horn neurons. J. Neurophysiol. 85, 1864–1872.

Gleason, C.E., Dowling, N.M., Wharton, W., Manson, J.E., Miller, V.M., Atwood, C.S., Brinton, E.A., Cedars, M.I., Lobo, R.A., Merriam, G.R., Neal-Perry, G., Santoro, N.F., Taylor, H.S., Black, D.M., Budoff, M.J., Hodis, H.N., Naftolin, F., Harman, S.M., Asthana, S., 2015. Effects of hormone therapy on cognition and mood in recently postmenopausal women: findings from the randomized, controlled KEEPS-cognitive and affective study. PLoS Med. 12, e1001833 (discussion e1001833).

Goosens, K.A., Maren, S., 2002. Long-term potentiation as a substrate for memory:

evidence from studies of amygdaloid plasticity and Pavlovian fear conditioning. Hippocampus 12, 592–599.
Gross, C., Santarelli, L., Brunner, D., Zhuang, X., Hen, R., 2000. Altered fear circuits in 5-HT(1A) receptor KO mice. Biol. Psychiatry 48, 1157–1163.
Gundersen, B.B., Briand, L.A., Onksen, J.L., Lelay, J., Kaestner, K.H., Blendy, J.A., 2013. Increased hippocampal neurogenesis and accelerated response to antidepressants in mice with specific deletion of CREB in the hippocampus: role of cAMP response-element modulator tau. J. Neurosci. 33, 13673–13685.
Gundlah, C., Alves, S.E., Clark, J.A., Pai, L.Y., Schaeffer, J.M., Rohrer, S.P., 2005. Estrogen receptor-beta regulates tryptophan hydroxylase-1 expression in the murine midbrain raphe. Biol. Psychiatry 57, 938–942.
Halbreich, U., Rojansky, N., Palter, S., Tworek, H., Hissin, P., Wang, K., 1995. Estrogen augments serotonergic activity in postmenopausal women. Biol. Psychiatry 37, 434–441.
Harlow, S.D., Gass, M., Hall, J.E., Lobo, R., Maki, P., Rebar, R.W., Sherman, S., Sluss, P.M., de Villiers, T.J., Group, S.C, 2012. Executive summary of the stages of reproductive aging workshop + 10: addressing the unfinished agenda of staging reproductive aging. J. Clin. Endocrinol. Metab. 97, 1159–1168.
Hiroi, R., Neumaier, J.F., 2011. Complex roles of estrogen in emotion: sex matters. Biol. Psychiatry 70, 908–909.
Hiroi, R., McDevitt, R.A., Neumaier, J.F., 2006. Estrogen selectively increases tryptophan hydroxylase-2 mRNA expression in distinct subregions of rat midbrain raphe nucleus: association between gene expression and anxiety behavior in the open field. Biol. Psychiatry 60, 288–295.
Itoh, T., Kajikuri, J., 2011. Characteristics of the actions by which 5-HT affects electrical and mechanical activities in rabbit jugular vein. Br. J. Pharmacol. 164, 979–991.
Jang, H.-J., Cho, K.-H., Park, S.-W., Kim, M.-J., Yoon, S.H., Rhie, D.-J., 2010. Effects of serotonin on the induction of long-term depression in the rat visual cortex. Korean J. Physiol. Pharmacol. 14, 337.
Khatri, N., Simpson, K.L., Lin, R.C., Paul, I.A., 2014. Lasting neurobehavioral abnormalities in rats after neonatal activation of serotonin 1A and 1B receptors: possible mechanisms for serotonin dysfunction in autistic spectrum disorders. Psychopharmacology 231, 1191–1200.
Kilkenny, C., Browne, W., Cuthill, I.C., Emerson, M., Altman, D.G., National Centre for the Replacement, R., Reduction of Amimals in, R, 2011. Animal research: reporting in vivo experiments–the ARRIVE guidelines. J. Cereb. Blood Flow Metab. 31, 991–993.
Kim, J., Lee, S., Park, K., Hong, I., Song, B., Son, G., Park, H., Kim, W.R., Park, E., Choe, H.K., Kim, H., Lee, C., Sun, W., Kim, K., Shin, K.S., Choi, S., 2007. Amygdala depotentiation and fear extinction. Proc. Natl. Acad. Sci. U. S. A. 104, 20955–20960.
Klemenhagen, K.C., Gordon, J.A., David, D.J., Hen, R., Gross, C.T., 2006. Increased fear response to contextual cues in mice lacking the 5-HT1A receptor. Neuropsychopharmacology 31, 101–111.
Kranz, G.S., Wadsak, W., Kaufmann, U., Savli, M., Baldinger, P., Gryglewski, G., Haeusler, D., Spies, M., Mitterhauser, M., Kasper, S., Lanzenberger, R., 2015. High-dose testosterone treatment increases serotonin transporter binding in transgender people. Biol. Psychiatry 78, 525–533.
Krezel, W., Dupont, S., Krust, A., Chambon, P., Chapman, P.F., 2001. Increased anxiety and synaptic plasticity in estrogen receptor beta -deficient mice. Proc. Natl. Acad. Sci. U. S. A. 98, 12278–12282.
Li, C., Rainnie, D.G., 2014. Bidirectional regulation of synaptic plasticity in the basolateral amygdala induced by the D1-like family of dopamine receptors and group II metabotropic glutamate receptors. J. Physiol. 592, 4329–4351.
Li, M., Sun, T., Zhang, C., Hu, G., 2010. Distinct neural mechanisms underlying acute and repeated administration of antipsychotic drugs in rat avoidance conditioning. Psychopharmacology 212, 45–57.
Maffucci, J., Gore, A., 2006. Age-related changes in hormones and their receptors in animal models of female reproductive senescence. In: Conn, M. (Ed.), Handbook of Models for Human Aging. Academic Press and Elsevier, San Diego, pp. 533–552.
Mark-Kappeler, C.J., Hoyer, P.B., Devine, P.J., 2011. Xenobiotic effects on ovarian preantral follicles. Biol. Reprod. 85, 871–883.
Mayer, L.P., Pearsall, N.A., Christian, P.J., Devine, P.J., Payne, C.M., McCuskey, M.K., Marion, S.L., Sipes, I.G., Hoyer, P.B., 2002. Long-term effects of ovarian follicular depletion in rats by 4-vinylcyclohexene diepoxide. Reprod. Toxicol. 16, 775–781.
Nejat, E.J., Chervenak, J.L., 2010. The continuum of ovarian aging and clinicopathologies associated with the menopausal transition. Maturitas 66, 187–190.
Pape, H.C., 2005. GABAergic neurons: gate masters of the amygdala, mastered by dopamine. Neuron 48, 877–879.
Pattij, T., Groenink, L., Oosting, R.S., van der Gugten, J., Maes, R.A., Olivier, B., 2002. GABA(a)-benzodiazepine receptor complex sensitivity in 5-HT(1A) receptor knockout mice on a 129/Sv background. Eur. J. Pharmacol. 447, 67–74.
Penington, N.J., Kelly, J.S., Fox, A.P., 1993. Whole-cell recordings of inwardly rectifying K+ currents activated by 5-HT1A receptors on dorsal raphe neurones of the adult rat. J. Physiol. 469, 387–405.
Pestana-Oliveira, N., Kalil, B., Leite, C.M., Carolino, R.O.G., Debarba, L.K., Elias, L.L.K., Antunes-Rodrigues, J., Anselmo-Franci, J.A., 2018. Effects of estrogen therapy on the serotonergic system in an animal model of perimenopause induced by 4-Vinylcyclohexen Diepoxide (VCD). eNeuro 5.
Prior, J.C., 2011. The endocrinology of perimenopause need for a paradigm shift. Front. Biosci. S3, 474–486.
Rainnie, D.G., 1999. Serotonergic modulation of neurotransmission in the rat basolateral amygdala. J. Neurophysiol. 82, 69–85.
Ramboz, S., Oosting, R., Amara, D.A., Kung, H.F., Blier, P., Mendelsohn, M., Mann, J.J., Brunner, D., Hen, R., 1998. Serotonin receptor 1A knockout: an animal model of anxiety-related disorder. Proc. Natl. Acad. Sci. U. S. A. 95, 14476–14481.
Rammes, G., Eder, M., Dodt, H.U., Kochs, E., Zieglgansberger, W., 2001. Long-term depression in the basolateral amygdala of the mouse involves the activation of interneurons. Neuroscience 107, 85–97.
Reis, F.M., Pestana-Oliveira, N., Leite, C.M., Lima, F.B., Brandao, M.L., Graeff, F.G., Del-Ben, C.M., Anselmo-Franci, J.A., 2014. Hormonal changes and increased anxiety-like behavior in a perimenopause-animal model induced by 4-vinylcyclohexene diepoxide (VCD) in female rats. Psychoneuroendocrinology 49, 130–140.
Rosenkranz, J.A., Grace, A.A., 1999. Modulation of basolateral amygdala neuronal firing and afferent drive by dopamine receptor activation in vivo. J. Neurosci. 19, 11027–11039.
Rousseau, M., 2006. Managing menopausal symptoms. In: Conn, M. (Ed.), Handbook of Models for Human Aging. Elsevier Academic Press, Amsterdam.
Sakai, N., Tanaka, C., 1993. Inhibitory modulation of long-term potentiation via the 5-HT1A receptor in slices of the rat hippocampal dentate gyrus. Brain Res. 613, 326–330.
Sanberg, C.D., Jones, F.L., Do, V.H., Dieguez Jr., D., Derrick, B.E., 2006. 5-HT1a receptor antagonists block perforant path-dentate LTP induced in novel, but not familiar, environments. Learn. Mem. 13, 52–62.
Sangha, S., Narayanan, R.T., Bergado-Acosta, J.R., Stork, O., Seidenbecher, T., Pape, H.C., 2009. Deficiency of the 65 kDa isoform of glutamic acid decarboxylase impairs extinction of cued but not contextual fear memory. J. Neurosci. 29, 15713–15720.
Santoro, N., Randolph Jr., J.F., 2011. Reproductive hormones and the menopause transition. Obstet. Gynecol. Clin. N. Am. 38, 455–466.
Schiapparelli, L., Del Rio, J., Frechilla, D., 2005. Serotonin 5-HT receptor blockade enhances ca(2+)/calmodulin-dependent protein kinase II function and membrane expression of AMPA receptor subunits in the rat hippocampus: implications for memory formation. J. Neurochem. 94, 884–895.
Schmitz, D., Gloveli, T., Empson, R.M., Heinemann, U., 1998. Serotonin reduces polysynaptic inhibition via 5-HT1A receptors in the superficial entorhinal cortex. J. Neurophysiol. 80, 1116–1121.
Toufexis, D.J., Myers, K.M., Davis, M., 2006. The effect of gonadal hormones and gender on anxiety and emotional learning. Horm. Behav. 50, 539–549.
Van Kempen, T.A., Milner, T.A., Waters, E.M., 2011. Accelerated ovarian failure: a novel, chemically induced animal model of menopause. Brain Res. 1379, 176–187.
Waider, J., Araragi, N., Gutknecht, L., Lesch, K.P., 2011. Tryptophan hydroxylase-2 (TPH2) in disorders of cognitive control and emotion regulation: a perspective. Psychoneuroendocrinology 36, 393–405.
Wang, X., Chang, F., Bai, Y., Chen, F., Zhang, J., Chen, L., 2014. Bisphenol a enhances kisspeptin neurons in anteroventral periventricular nucleus of female mice. J. Endocrinol. 221, 201–213.
Wang, X., Bai, Y., Tang, C., Cao, X., Chang, F., Chen, L., 2018. Impact of Perfluorooctane sulfonate on reproductive ability of female mice through suppression of estrogen receptor alpha-activated Kisspeptin neurons. Toxicol. Sci. 165, 475–486.
Wu, L.J., Kim, S.S., Zhuo, M., 2008. Molecular targets of anxiety: from membrane to nucleus. Neurochem. Res. 33, 1925–1932.
Yang, R., Zhang, B., Chen, T., Zhang, S., Chen, L., 2017. Postpartum estrogen withdrawal impairs GABAergic inhibition and LTD induction in basolateral amygdala complex via down-regulation of GPR30. Eur. Neuropsychopharmacol. 27, 759–772.
Yuen, E.Y., Jiang, Q., Chen, P., Gu, Z., Feng, J., Yan, Z., 2005. Serotonin 5-HT1A receptors regulate NMDA receptor channels through a microtubule-dependent mechanism. J. Neurosci. 25, 5488–5501.
Yuen, E.Y., Jiang, Q., Chen, P., Feng, J., Yan, Z., 2008. Activation of 5-HT2A/C receptors counteracts 5-HT1A regulation of n-methyl-D-aspartate receptor channels in pyramidal neurons of prefrontal cortex. J. Biol. Chem. 283, 17194–17204.
Zajac, M.S., Renoir, T., Perreau, V.M., Li, S., Adams, W., van den Buuse, M., Hannan, A.J., 2018. Short-term environmental stimulation spatiotemporally modulates specific serotonin receptor gene expression and behavioral pharmacology in a sexually dimorphic manner in Huntington's disease transgenic mice. Front. Mol. Neurosci. 11, 433.
Zhang, B., Wang, L., Chen, T., Hong, J., Sha, S., Wang, J., Xiao, H., Chen, L., 2017. Sigma-1 receptor deficiency reduces GABAergic inhibition in the basolateral amygdala leading to LTD impairment and depressive-like behaviors. Neuropharmacology 116, 387–398.